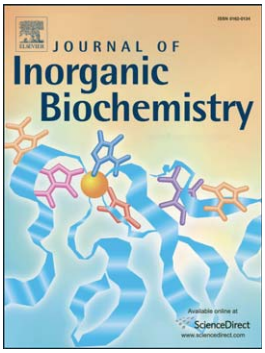

Ru(II)-based complexes with *N*-(acyl)-*N'*,*N'*-(disubstituted)thiourea ligands: Synthesis, characterization, BSA- and DNA-binding studies of new cytotoxic agents against lung and prostate tumour cells

Rodrigo S. Correa, Katia M. de Oliveira, Fábio G. Delolo, Anislay Alvarez, Raúl Mocelo, Ana M. Plutin, Marcia R. Cominetti, Eduardo E. Castellano, Alzir A. Batista

PII: S0162-0134(15)00102-6
DOI: doi: 10.1016/j.jinorgbio.2015.04.008
Reference: JIB 9708

To appear in: *Journal of Inorganic Biochemistry*

Received date: 14 January 2015
Revised date: 12 April 2015
Accepted date: 13 April 2015

Ru(II)-based complexes with *N*-(acyl)-*N*',*N*'-(disubstituted)thiourea ligands: synthesis, characterization, BSA- and DNA-binding studies of new cytotoxic agents against lung and prostate tumour cells

Rodrigo S. Correa[a,*], Katia M. de Oliveira[a], Fábio G. Delolo[a], Anislay Alvarez[b], Raúl Mocelo[b], Ana M. Plutin[b], Marcia R. Cominetti[c], Eduardo E. Castellano[d], Alzir A. Batista[a,*]

[a] Departamento de Química, Universidade Federal de São Carlos – UFSCar, Rodovia Washington Luís KM 235, CP 676, 13561-901, São Carlos, SP, Brazil; [b]Laboratório de Síntesis Orgánica, Facultad de Química, Universidad de la Habana, Habana 10400, Cuba. [c]Departamento de Gerontologia, Universidade Federal de São Carlos, São Carlos, SP, Brazil; [d]Departamento de Física e Informática, Instituto de Física de São Carlos, Universidade de São Paulo, CP 369, 13560-970, São Carlos, SP, Brazil.

Corresponding authors: Rodrigo S. Correa (rodricorrea@ufscar.br). Alzir A. Batista (daab@ufscar.br). Tel.: +55 1633518285; Fax: +55 1633518350.

Abstract

Four ruthenium(II)-based complexes with *N*-(acyl)-*N',N'*-(disubstituted)thiourea derivatives (Th) were obtained. The compounds, with the general formula *trans*-$[Ru(PPh_3)_2(Th)(bipy)]PF_6$, interact with bovine serum albumin (BSA) and DNA. BSA-binding constants, which were in the range of 3.3–6.5 x 10^4 M^{-1}, and the thermodynamic parameters (ΔG, ΔH and ΔS), suggest spontaneous interactions with this protein by electrostatic forces due to the positive charge of the complexes. Also, binding constant by spectrophotometric DNA titration (Kb = 0.8–1.8 x 10^4 M^{-1}) and viscosity studies indicate weak interactions between the complexes and DNA. Cytotoxicity assays against DU-145 (prostate cancer) and A549 (lung cancer) tumour cells revealed that the complexes are more active in tumour cells than in normal (L929) cells, and that they present high cytotoxicity (low IC_{50} values) compared with the reference metallodrug, cisplatin.

Keywords: Ruthenium/phosphine/diimine complexes, acylthiourea ligands, prostate cancer, lung cancer, DNA binding; BSA binding.

1. Introduction

In recent years, ruthenium(II) complexes have attracted attention due to their wide variety of structures, reactivities and applications, in particular those compounds with catalytic and anticancer activities [1-3]. Many research groups are exploring ruthenium complexes containing specific molecular fragments in order to design new bioactive anticancer metallodrugs, such as ruthenium/arene [4–5] and ruthenium/staurosporine analogues [6], and some of these are in early preclinical trials [7]. In the last ten years, our research group has investigated the reactivity and biological properties of ruthenium complexes containing phosphine and diimine ligands, which exhibit antitubercular, antitumour, antileishmanial and antiplasmodial activities [8-11]. Therefore, as part of our ongoing effort to design new bioactive metallodrug candidates, in this paper we used O,S-chelating acylthiourea ligands to synthesize a new phosphine/diimine/ruthenium(II) class of compounds with biological properties.

Thiourea derivatives were employed as an ionophore in amperometric sensors for Cd(II) [12], and they can be included in the field of coordination chemistry as versatile ligands. Conformational isomerism, steric effects and the presence of donor sites in their structures can provide several possible coordination modes [13, 14]. Usually, *N*-(acyl)-*N',N'*-(disubstituted)thiourea ligands form very stable complexes with a six-membered ring, presenting different complex:ligand stoichiometry, such as 1:2 or 1:3, according to the coordination number of the metal ion. Recently, we have explored the ability of *N*-acyl-*N'*,*N'*-disubstituted thiourea derivatives to form 1:3 and 1:2 stable complexes with transition metals, specifically with Co(III), Ni(II) and Cu(II) [15-20]. In such metal complexes, the acylthiourea derivatives acted as anionic O,S-chelating ligands with a *cis* configuration. In addition, neutral acylthiourea derivatives can also bind the metal centre as monodentate ligands through

the sulfur atom, such as observed in Cd(II) [21] and Cu(I) complexes [22]. Within the scope of coordination chemistry, a wide range of *d*-block metals with different oxidation states were synthesized with this type of ligand, presenting different modes of coordination [15-34]. Some of these complexes exhibited cytotoxicity against tumour cells, and were more cytotoxic than the free ligands [27-32]. Furthermore, catalytic [33] and luminescent [34] properties of this kind of complex were attributed to the presence of acylthiourea derivatives as ligands. Despite the fact that acylthioureas have been used frequently as ligands for syntheses of transition metal complexes, only two ruthenium(III) complexes [32, 35] have been investigated so far, and just one has been studied by X-ray diffraction. Thus, here we present the first report on ruthenium(II)/triphenylphosphine/2,2'-bipyridine complexes containing acylthiourea derivatives as the ligand. We describe here the synthesis, characterization, and X-ray crystallographic and biological studies of complexes containing one acylthiourea ligand per ruthenium(II) ion, which is different to the previously reported complexes that contained ruthenium(III) [32, 35].

The Figure 1 illustrates the structure of the four 1-(acyl)-3,3-(disubstituted)thiourea derivatives used as ligands [*N*-benzoyl-*N',N'*-diphenylthiourea ($BzPh_2Th$), *N*-(2-furoyl)-*N',N'*-diphenylthiourea ($FuPh_2Th$), *N*-benzoyl-*N',N'*-dibenzylthiourea ($BzBn_2Th$) and *N*-(2-furoyl)-*N',N'*-dibenzylthiourea ($FuBn_2Th$)]. In this paper, the metal/DNA and metal/albumin binding ability was also evaluated. Cytotoxic studies on a prostate tumour cell line [DU-145 (ATCC: HTB-81)], lung tumour cells [A549 (CCL-185)] and the L929 normal cell line were carried out.

INSERT FIGURE 1

2. Material and Methods

2.1 Materials, measurements and methods

All manipulations involving solutions of the complexes were performed under argon. All solvents used in the work were purified by standard methods. Chemicals used were of reagent grade or comparable purity. The $RuCl_3.3H_2O$, triphenylphosphine (PPh_3), 2,2'-bipyridine (bipy) and reagents used in the syntheses of acylthiourea derivatives (benzoyl chloride, furoyl chloride, dibenzylamine, diphenylamine and KSCN) were used as received from Aldrich. The *cis*-$[RuCl_2(bipy)(PPh_3)_2]$ complex was prepared according to the published procedure [36].

The IR spectra were recorded on a FT-IR Bomem-Michelson 102 spectrometer in the range 4000–250 cm^{-1} using CsI pellets. Conductivity data (presented as μS/cm) were obtained in CH_2Cl_2 using a Micronal model B-330 connected to a Pt with constant cell equal to 0.089 cm^{-1}; measurements were made at room temperature using 1 mM solutions of the complexes. ^1H and ^{13}C NMR spectra were recorded on a Bruker DRX 400 MHz, internally referenced to TMS (tetramethylsilane), chemical shift (δ), multiplicity (*m*), spin-spin coupling constant (*J*), and integral (*I*). $CDCl_3$ was used as solvent. The $^{31}P\{^1H\}$ chemical shifts are reported in relation to H_3PO_4 (85% v/v). The UV-Vis spectra of the complexes in CH_2Cl_2 were recorded on a Hewlett Packard diode array–8452A. Cyclic voltammetry experiments were carried out at 25 ºC in CH_2Cl_2 containing 0.10 M Bu4NClO4 (tetrabutylammonium perchlorate, TBAP) (Fluka Purum), with a BAS-100B/W Bioanalytical Systems Inc. electrochemical analyser. The working and auxiliary electrodes were stationary Pt foils; a Luggin capillary probe was used and the reference electrode was Ag/AgCl. Under these conditions, the ferrocene (Fc) is oxidized at 0.43 V (Fc^+/Fc). The microanalyses were performed in the Microanalytical

Laboratory of the Chemistry Department of the Federal University of São Carlos, with an EA 1108 CHNS microanalyser (Fisons Instruments).

2.2 Synthesis

The acylthiourea ligands were prepared using a standard procedure [13] by reacting the benzoyl/furoyl chloride with KSCN in anhydrous acetone, followed by condensation with dibenzylamine/diphenylamine. The reaction mixture was poured into cold water, resulting in precipitation of a solid, which was purified by recrystallization from acetone–water solution (1:1 *v/v*). The identity of the products was confirmed by comparing their infrared, ^{1}H and ^{13}C NMR data with those reported in the literature [13–21].

To obtain the complexes (1–4), the acylthiourea derivative (0.12 mmol) was dissolved in a Schlenk flask in 50 mL of a mixture of dichloromethane/methanol (2:1 *v/v*) with 20 μL of triethylamine and KPF_6 (0.12 mmol; 15.0 mg). Next, as the precursor, 100 mg (0.11 mmol) of the *cis*-$[RuCl_2(PPh_3)_2(bipy)]$ (chlorines in the *cis* position to each other, and PPh_3 in the *trans* position to each other) was added. The solution was kept under reflux, under an inert atmosphere and with stirring for 24 h. For each reaction, the final solution was concentrated to *ca.* 2 mL, and 10 mL of water was added to precipitate an orange powder. The solids were filtered off, washed with warm water, diethyl ether separately, and dried under *vacuum*.

N-benzoyl-*N',N'*-diphenylthiourea ($BzPh_2Th$) [$C_{20}H_{16}N_2OS$]: exp. (cal) C, 72.26 (72.19); H, 4.85 (4.80); N, 8.43 (8.40); S, 9.64 (9.59). Yield: 81 %: m.p. (ºC): 205-206 . IR (cm^{-1}): (νN-H) 3150; (νC-H) 3000, 2910; (νC=O) 1680; (νC=C) 1610; (I, N-C=S) 1520; (II, N-C=S) 1350; (III, N-C=S) 1160; (IV, N-C=S) 930. ^{1}H NMR (400 MHz, $CDCl_3$, 298 K): δ(ppm) 8.73 (hydrogen atom of N-H), 7.60-6.92 (15 hydrogen atoms of Ph). ^{13}C NMR (100 MHz, $CDCl_3$, 298 K): δ(ppm) 182.49 (C=S); 162.34 (C=O); 145.73, 143.15, 132.84, 132.73-117.82 (C-Ph). UV-Visible (UV-Vis) (CH_2Cl_2, 10^{-5} M): λ/nm (ε/$M^{-1}cm^{-1}$) 248 (18,252), 265 (17,475).

N-(2-furoyl)-*N',N'*-diphenylthiourea ($FuPh_2Th$) [$C_{18}H_{14}N_2O_2S$]: exp. (cal) C, 67.06 (67.00); H, 4.38 (4.33); N, 8.69 (8.65); S, 9.94 (9.90). Yield: 73 %: m.p. (ºC): 126-128. IR (cm^{-1}): (νN-H) 3120; (νC-H) 3005, 2910; (νC=O) 1690; (νC=C) 1615; (I, N-C=S) 1530; (II, N-C=S) 1325; (III, N-C=S) 1163; (IV, N-C=S) 1025. ^{1}H NMR (400 MHz, $CDCl_3$, 298 K): δ(ppm) 8.91 (hydrogen atom of N-H), 7.44 -6.49 (13 hydrogen atoms of Ph and Fu). ^{13}C NMR (100 MHz, $CDCl_3$, 298 K): δ(ppm) 183.06(C=S); 153.40 (C=O); 146.87, 145.78, 145.52, 144.96-116.58 (C-Ph) and 113.55-111.73 (C-Fu). UV-Vis (CH_2Cl_2, 10^{-5} M): λ/nm (ε/$M^{-1}cm^{-1}$) 235 (13,750), 284 (23,000).

N-benzoyl-*N',N'*-dibenzylthiourea ($BzBn_2Th$) [$C_{22}H_{20}N_2OS$]: exp. (cal) C, 73.30 (72.89); H, 5.59 (5.48); N, 7.77 (7.71); S, 8.89 (8.82). Yield: 83 %: m.p. (ºC): 136-138. IR (cm^{-1}): (νN-H) 3330; (νC-H) 3000, 2900; (νC=O) 1690; (νC=C) 1583; (I, N-C=S) 1514; (II, N-C=S) 1355; (III, N-C=S) 1192; (IV, N-C=S) 932. ^{1}H NMR (400 MHz, $CDCl_3$, 298 K): δ(ppm) 8.58 (N-H), 7.80-7.11 (15H of Ph), 5.23 and 4.72 (4H of $2CH_2$). ^{13}C NMR (100 MHz, $CDCl_3$, 298 K): δ(ppm) 181.94 (C=S); 163.95 (C=O); 135.38, 134.67, 133.10, 132.48-127.90 (C-Ph), 56.73 and 56.00 ($2CH_2$). UV-Vis (CH_2Cl_2, 10^{-5} M): λ/nm (ε/$M^{-1}cm^{-1}$) 257 (12,484), 321 (12,725).

N-(2-furoyl)-*N',N'*-dibenzylthiourea ($FuBn_2Th$) [$C_{20}H_{18}N_2O_2S$]: exp. (cal) C, 68.55 (68.49); H, 5.18 (5.04); N, 7.99 (7.93); S, 9.15 (9.08). Yield: 76 %: m.p. (ºC): 146-147. IR (cm^{-1}): (νN-H) 3320; (νC-H) 3020, 2905; (νC=O) 1693; (νC=C) 1608; (I, N-C=S) 1580; (II, N-C=S) 1425; (III, N-C=S) 1173; (IV, N-C=S) 1020. ^{1}H NMR (400 MHz, $CDCl_3$, 298 K): δ(ppm) 8.72 (N-H), 7.53-6.56 (13 H of Ph and Fu). ^{13}C NMR (100 MHz, $CDCl_3$, 298 K): δ(ppm) 180.83(CS); 153.95 (CO); 146.11, 145.59, 135.25, 134.59-127.79 (C-Ph); 117.66-113.00 (C-Fu) and 56.22 ($2CH_2$). UV-Vis (CH_2Cl_2, 10^{-5} M): λ/nm (ε/$M^{-1}cm^{-1}$) 237 (9,760), 275 (19,337).

trans-[$Ru(PPh_3)_2(BzPh_2Th)(bipy)]PF_6$ (1): Yield: 120 mg (81%). Anal. Calc. for $[RuC_{66}H_{53}N_4OP_2S]PF_6$: exp. (calc) C, 63.05 (63.00); H, 4.27 (4.25); N, 4.31 (4.45); S, 2.62 (2.55) %. Molar conductance (μS/cm, CH_2Cl_2) 54.1. IR (cm^{-1}): ($\nu CH_{PPh3,\ bipy,\ Th}$) 3078, 3055, 2922, 2853; ($\nu C{=}N_{bipy}$) 1603; (νC=O) 1588; (νC=C and νC=N) 1500, 1489, 1489, 1479, 1435, 1402, 1356; (νC-S) 1294; ν-P) 1090; (ν_{ring}) 1072, 1024, 1001; (νP-F) 841; (γC=S) 764; (νRu-P) 517, (νRu-S) 492; (νRu-N) 403; (νRu-O) 355. $^{31}P\{^1H\}$ NMR (162 MHz, $CDCl_3$, 298 K): δ(ppm) 21.12 (s). ^1H NMR (400 MHz, $CDCl_3$, 298 K): δ(ppm) 9.21 and 8.16 (2H, C-H of bipy adjacent to the coordinated nitrogen atoms); 7.88-6.74 (30H atoms of PPh_3, 15H aromatic of $BzPh_2Th$ and 6H aromatic of bipy). ^{13}C NMR (100 MHz, $CDCl_3$, 298 K): δ(ppm) 177.36 (C=S); 172.59 (C=O); 158.74, 157.07, 153.56, 151.87, 151.18, 148.70, 145.11, 138.54, 136.13, 135.76, 133.28 – 123.37 (C-Ph; C-bipy, C-PPh_3). UV-Vis (CH_2Cl_2, 10^{-5} M): λ/nm (ε/$M^{-1}cm^{-1}$) 281 (4820), 407 (903), 476 (664).

trans-[$Ru(PPh_3)_2(FuPh_2Th)(bipy)]PF_6$ (2): Yield: 135 mg (89%). Anal. Calc. for $[RuC_{64}H_{53}N_4O_2P_2S]PF_6$: exp. (calc) C, 61.50(61.49); H, 3.97(4.27); N, 4.24(4.48); S, 2.34 (2.56) %. Molar conductance (μS/cm, CH_2Cl_2) 56.1. IR (cm^{-1}): ($\nu CH_{PPh3,\ bipy,\ Th}$) 3080, 3059, 2922, 2852; ($\nu C{=}N_{bipy}$) 1603; (νC=O) 1578; ($\nu C{=}C_{furoyl}$) 1512; (νC=N and νC=C) 1491,1481, 1471, 1456, 1435, 1418, 1391, 1358; (νCS) 1292; (νC-P) 1090; (ν_{ring}) 1072, 1026, 999; (νP-F) 841; (γCS) 766; (νRu-P) 520; (νRu-S) 496; (νRu-N) 403; (νRu-O) 357. $^{31}P\{^1H\}$ NMR (162 MHz, $CDCl_3$, 298 K): δ(ppm) 21.95 (s). ^1H NMR (400 MHz, $CDCl_3$, 298 K): δ(ppm) 9.40 and 8.25 (2H, C-H of bipy adjacent to the coordinated nitrogen atoms); 7.94-6.28 (30H aromatic hydrogen atoms of PPh_3, 13H aromatic hydrogen atoms of $FuPh_2Th$ and 6H aromatic hydrogen atoms of bipy). ^{13}C NMR (100 MHz, $CDCl_3$, 298 K): δ(ppm) 176.36 (CS); 165.05 (CO); 159.59, 158.95, 156.93, 153.30, 149.53, 148.92, 145.37, 144.93, 135.81-122.88 (C-Ph; C-bipy, C-PPh_3), 117.81-111.84 (C-Furoyl). UV-Vis (CH_2Cl_2, 10^{-5} M): λ/nm (ε/$M^{-1}cm^{-1}$) 282 (3540), 406 (900), 472 (706).

trans-[Ru(PPh_3)$_2$($BzBn_2Th$)(bipy)]PF_6 (3): Yield: 95 mg (65%). Anal. Calc. for [$RuC_{68}H_{57}N_4OP_2S$]PF_6: exp. (calc) C, 61.60(61.59); H, 4.37(4.12); N, 4.77(4.49); S, 2.38 (2.57) %. Molar conductance (μS/cm, CH_2Cl_2) 57.0. IR (cm^{-1}): ($\nu CH_{PPh3,\ bipy,\ Th}$) 3080, 3059, 3028, 2922, 2853; ($\nu C{=}N_{bipy}$) 1603; (νC=O) 1585; (νC=N and νC=C) 1508, 1495, 1481, 1470, 1450, 1433, 1412, 1400, 1354; (νCS) 1267; (δCH_2) 1207; (νC-P) 1088; (ν_{ring}) 1072, 1028, 1001; (νP-F) 839; (γCS) 758; (νRu-P) 521; (νRu-S) 490; (νRu-N) 405; (νRu-O) 360. $^{31}P\{^1H\}$ NMR (162 MHz, $CDCl_3$, 298 K): δ(ppm) 22.07 (s). ^1H NMR (400 MHz, $CDCl_3$, 298 K): δ(ppm) 9.26 and 8.48 (2H, C-H of bipy adjacent to the coordinated nitrogen atoms); 7.83-6.98 (30H aromatic hydrogen atoms of PPh_3, 15H aromatic hydrogen atoms of $BzBn_2Th$ and 6H aromatic hydrogen atoms of bipy); 4.95 and 4.74 (4H, CH_2 of $BzBn_2Th$). ^{13}C NMR (100 MHz, $CDCl_3$, 298 K): δ(ppm) 176.55 (CS); 173.02 (CO); 158.94, 157.18, 153.56, 148.59, 139.02-123.47 (C-Ph; C-bipy, C-PPh_3), 53.41 and 51.60 (CH_2). UV-Vis (CH_2Cl_2, 10^{-5} M): λ/nm (ε/$M^{-1}cm^{-1}$) 279 (2676), 392 (546), 483 (367).

trans-[Ru(PPh_3)$_2$($FuBn_2Th$)(bipy)]PF_6 (4): Yield: 110 mg (74%). Anal. Calc. for [$RuC_{66}H_{57}N_4O_2P_2S$]PF_6: exp. (calc) C, 62.34(62.11); H, 4.70(4.34); N, 4.54(4.39); S, 2.28 (2.51) %. Molar conductance (μS/cm, CH_2Cl_2) 56.5. IR (cm^{-1}): ($\nu CH_{PPh3,\ bipy,\ Th}$) 3080, 3059, 3028, 2924, 2854; ($\nu C{=}N_{bipy}$) 1605; (νC=O) 1578; ($\nu C{=}C_{furoyl}$) 1522; (νC=N and νC=C) 1495, 1481, 1466, 1452, 1433, 1416, 1383, 1356, 1309; (νC-S) 1267; (δCH_2) 1211; (νC-P) 1090; (ν_{ring}) 1080, 1028, 1001; (νP-F) 843; (γC=S) 762; (νRu-P) 518; (νRu-S) 494; (νRu-N) 401; (νRu-O) 353. $^{31}P\{^1H\}$ NMR (162 MHz, $CDCl_3$, 298 K): δ(ppm) 22.49 (s). ^1H NMR (400 MHz, $CDCl_3$, 298 K): δ(ppm) 9.41 and 8.54 (2H, C-H of bipy adjacent to the coordinated nitrogen atoms); 7.42-6.45 (30H atoms of PPh_3, 13H aromatic atoms of $FuBn_2Th$ and 6H aromatic atoms of bipy); 4.90 and 4.56 (4H, CH_2 of $FuBn_2Th$). ^{13}C NMR (100 MHz, $CDCl_3$, 298 K): δ(ppm) 175.53 (CS); 164.70 (CO); 159.18, 157.07, 153.49, 148.56, 145.09, 137.24-

123.59 (C-Ph; C-bipy, C-PPh_3), 113.23-111.80 (C-Furoyl), 52.95 and 51.36 (CH_2). UV-Vis (CH_2Cl_2, 10^{-5} M): λ/nm (ε/$M^{-1}cm^{-1}$) 280 (2035), 392 (497), 480 (351).

2.3 X-ray structure determination

Orange single-crystals of the complexes 1–4 were grown from diethyl ether diffusion into a dichloromethane solution of the complex. Room temperature (298 K) X-ray diffraction experiments were carried out using a suitable crystal mounted on glass fibre and positioned on the goniometer head. Intensity data were measured on an Enraf–Nonius Kappa-CCD diffractometer with graphite monochromated MoKα radiation (λ = 0.71073 Å). The cell refinements were performed using the software Collect [37] and Scalepack [38], and the final cell parameters were obtained on all reflections. Data reduction was carried out using the software Denzo-SMN and Scalepack [38]. The structures were solved by the direct method using SHELXS-97 [39] and refined using the software SHELXL-97 [39]. The Gaussian method was used for the absorption corrections [40]. Non-hydrogen atoms of the complexes were unambiguously located, and a full-matrix, least-squares refinement of these atoms with anisotropic thermal parameters was carried out. In all ligands of the complexes 1–4, the aromatic C–H hydrogen atoms were positioned stereochemically and were refined with fixed individual displacement parameters [$U_{iso}(H) = 1.2\ U_{eq}(Csp^2)$] using a riding model with aromatic C–H bond lengths fixed at 0.93 Å. Methylene groups of the $BzBn_2Th$ and $FuBn_2Th$ ligands in complexes 3 and 4 were also set as isotropic with a thermal parameter 20% greater than the equivalent isotropic displacement parameter of the atom to which each one was bonded, and C–H bond lengths were fixed at 0.97 Å. Tables and structure representations were generated by WinGX [41] and MERCURY [42], respectively. The main crystal data collections and structure refinement parameters for 1–4 are summarized in Table 1.

INSERT TABLE 1

2.4 Bovine serum albumin binding experiments

The protein binding study was performed by a tryptophan fluorescence quenching experiment using bovine serum albumin (BSA, 2.5 μM) in buffer (4.5 mM Tris-HCl, 0.5 mM NaOH, 50 mM NaCl) at pH 7.4. The extinction of the emission intensity of the tryptophan residue at 340 nm (excitation wavelength of 280 nm) was monitored using the complexes as suppressors in different concentrations (0–100 μM) in DMSO. Fluorescence spectra were recorded from 300 to 500 nm and performed in triplicate, using an opaque 96-well plate. Fluorescence spectra were recorded on a SpectraMax M3 at different temperatures (295 and 310 K).

2.5 DNA titration and viscosity experiments

A standard solution of calf thymus DNA (ctDNA) from Sigma-Aldrich was prepared in Tris-HCl buffer (5 mM Tris-HCl, pH 7.2). The concentration of this ctDNA solution was measured from its absorption intensity at 260 nm using the molar absorption coefficient value of 6600 M^{-1} cm^{-1}. The ctDNA solution is protein-free, given that the ratio of UV absorbance at 260 and 280 nm is about 1.8:1. The solution of ruthenium complexes 1–4 used in the experiments was prepared in Tris-HCl buffer containing 2% DMSO. In the titration experiments, different concentrations of the ctDNA were used while the ruthenium complex was at 25 μM. Sample correction was made for the absorbance of ctDNA and the spectra were recorded after solution equilibration for 1 min. The intrinsic equilibrium binding constant (Kb) of the complexes to ctDNA was obtained by monitoring changes in the absorption intensity with increasing concentration of ctDNA, and was analysed by regression analysis.

Viscosity experiments were carried out using an Ostwald viscometer maintained at a constant temperature of 25 °C in a thermostatic bath. The viscosity of the DNA solution was measured in the presence of increasing amounts of the complexes (1–4).

The flow times were measured with an automated timer. Each sample was measured three times, and an average flow time was calculated. The obtained data are presented as $(\eta/\eta_0)^{1/3}$ versus *r*, where η is the viscosity of DNA in the presence of the complexes, and η_0 is the viscosity of DNA alone in buffer solution [43–46].

2.6 Cell culture assay

The cytotoxic activities of ruthenium complexes 1–4 were evaluated against the human prostate tumour cell line DU-145 (ATCC: HTB-81) and against lung tumour A549 (CCL-185) cells. For initial screening of antitumour candidates, the *in vitro* assays were performed using the MTT (3-(4,5-dimethylthiazol-2-yl)-2,5-diphenyltetrazolium bromide) method, a colorimetric assay in which the mitochondria of viable cell reduct the soluble yellow tetrazolium salt to blue formazan crystals [47]. The A549 cells were maintained in Dulbecco's modified Eagle's medium (DMEM) and the DU-145 and L929 (ATCC: CCL-1) cells were maintained in RPMI-1640 medium. All cell lines were supplemented with 10% of foetal bovine serum (FBS), at 37 ºC in a humidified 5% CO_2 atmosphere. After reaching confluence, cells were detached by trypsinization and 1.5×10^4 cells/well were seeded in 200 μL of complete medium in 96-well assay microplates. The plates were incubated at 310 K in 5% CO_2 for at least 12 h to allow cell adhesion prior to compound testing. All tested compounds were dissolved in sterile DMSO (stock solution with maximum concentration of 20 mM) and diluted to 100 to 0.05 μM (final concentration in each well), where 1 μL aliquots were added to 200 μL of medium (final concentration of 0.5% DMSO/well). Cells were incubated with compounds for 48 h at 310 K in 5% CO_2.

In order to verify the cytotoxic effect of the complexes, the cell viability was measured after incubation with the complexes. Cells were twice washed with phosphate buffered saline (PBS) and MTT solution (0.5 mg/mL, 50 μL/well) was added to cells and incubated for 4 hours, after which 100 μL of isopropanol was added to dissolve the precipitated formazan crystals. The conversion of MTT to formazan by metabolically viable cells was measured in an automated microplate reader at 595 nm. To analyse the cell viability, the control (cells with only DMSO) was taken as the reference (100%). All experiments were carried out in triplicate. The percentage of viable cells was calculated as the mean with respect to the DMSO control. The IC_{50} (drug concentration at which 50% of the cells are viable relative to the control) values were obtained by non-linear fitting using GraphPad Prism software.

3. Results and Discussion

3.1 Synthesis

The reactions of *cis*-[$RuCl_2(PPh_3)_2$(bipy)] with *N*-Acyl-*N'*,*N'*-disubstituted thiourea derivatives (Th) produce complexes with the general formula [$Ru(PPh_3)_2$(Th)(bipy)]PF_6, in which the *N*-acyl-*N'*,*N'*-disubstituted thiourea ligand is chelated and negatively charged. The synthetic step used in this work was straightforward and with good yield, providing satisfactory elemental analysis data. The molar conductance measurements for compounds (1–4) were carried out in dichloromethane, and the results, ranging 54.1–57.0 μS/cm, are consistent with 1:1 type compounds [48].

3.2 Crystal structure and molecular assembly analysis of complexes 1–4

The X-ray studies confirm the structures proposed for the complexes: *trans*-[$Ru(PPh_3)_2(BzPh_2Th)(bipy)]PF_6$ (1), *trans*-[$Ru(PPh_3)_2(FuPh_2Th)(bipy)]$ PF_6 (2), *trans*-[$Ru(PPh_3)_2(BzBn_2Th)(bipy)]PF_6$ (3), and *trans*-[$Ru(PPh_3)_2(FuBn_2Th)(bipy)]PF_6$ (4) (Fig. 2 and Fig. S4, supplementary information). The complexes present one acylthiourea derivative, one 2,2'-bipyridine, and two triphenylphosphine ligands, forming slightly distorted octahedral geometries, highlighted by the bond angles around the metal centres (Table 3). The N–Ru–N bond angles on the equatorial position are far from the expected value of 90° due to the tension of the five-membered chelate ring of the bipy, while the six-membered ring formed by the acylthiourea derivatives ligands are less tensioned, presenting values close to 90°. The P–Ru–N and P1–Ru–P2 (PPh_3 ligands adopting a *trans* configuration) bond angles are close to 90° and 180°, respectively (Table 3). Ru–N_{bipy} and Ru–P_{PPh3} bond lengths found in complexes 1–4 are in agreement with values present in complexes obtained from the same Ru(II) precursor [11, 49].

INSERT FIGURE 2

INSERT TABLE 3

The crystal structures of two free ligands, $FuBn_2Th$ [50] and $BzBn_2Th$ [51], were previously published. In the free ligands, the C2=S1 (1.661–1.676 Å) and C1=O1 (1.214–1.215 Å) bond lengths indicate a double-bond character, whereas the C1–N1 and C2–N1 bonds are single (1.373–1.412 Å). As a result of acylthiourea coordination, the bond lengths present significant C2–S1 and C1–O1 lengthening and C–N shortening (Table 3).

The conformation between the thiocarbonyl and the carbonyl groups of metal-free ligands is twisted [50, 51, 52]. After coordination, the conformation of the *N'N'*-dibenzyl group changed significantly. In the $BzBn_2Th$ and $FuBn_2Th$ free ligands, the torsion angles

between the two benzyl groups are 108º and 104º, respectively, whereas in the complexes 3 and 4, the torsion angles are similar with values close to -153º. The planarity of the acylthiourea moiety is highlighted by the dihedral angle between the planes passing through the N1–C1–O1–C3 atoms and N1–C2–S2–N2 atoms. For the complexes 1, 2, 3 and 4, the dihedral angles are 1.51º, 7.84º, 5.44º and 10.16º, respectively, suggesting that the *N*-furoyl groups, as well as the *N',N'*-dibenzyl groups, contribute to distorting the coordinated acylthiourea moiety. This result is also supported by analysing the torsion angle of the acylthiourea moiety, in which the C1—N1—C2—S1 fragment tends to be more distorted than the O1—C1—N1—C2 fragment, particularly in complexes 2–4 (Table 3).

In the crystal structure of complexes 2 and 4, the oxygen atom of the furan group presents a *syn* conformation related to the oxygen of the coordinated carbonyl. The conformation adopted by the furan is allowed due to the weak intramolecular interaction between the C–H groups of the PPh_3 or bipy ligands with the oxygen of furan (Fig. S8, supplementary information).

The crystal structure of free ligands $BzBn_2Th$ and $FuBn_2Th$ exhibit patterns with N−H…S and C−H…O interactions forming infinite chains [50, 51]. However, in the complexes (1–4), both sulfur and oxygen atoms are coordinated and the N–H group is absent. Therefore, to stabilize the crystal structure of the complexes 1–4, there are only weak C–H…F–P intermolecular interactions, as well as van der Waals forces and π–π stacking, which can be mapped using the Hirshfeld surface and the fingerprint plots analysis (Fig. S5 and S6, supplementary information). It is well known that the non-classical interactions can provide good structural motifs for the construction of extended architectures and can stabilize the crystal structures of metal complexes with acylthiourea derivatives [15, 20, 53, 54]. These intermolecular interactions may be responsible for binding the complex to biological targets.

3.3 Infrared and ultraviolet-visible spectroscopy

In the IR spectra of complexes 1–4, the *ν*N–H stretching band, at around 3200 cm^{-1}, is not present, suggesting that the coordinated ligand is deprotonated. The free ligands present an intense band in the region between 1800 and 1610 cm^{-1}, which is assigned to *ν*C=O stretching vibrations [28, 29, 55] and is absent in the spectra of the complexes, evidencing that upon the ligand coordination, the carbonyl absorption shifts to lower frequencies around 1575–1590 cm^{-1}. Strong bands in the region of 1550-1300 cm^{-1} are characteristic of *ν*C=N and *ν*C=C stretching vibrations and are present in the spectra of the ligands and of the complexes. In the complexes, the bands related to νC⎓S and δC⎓S absorptions occur in the regions around 1260 and 760 cm^{-1}, respectively. The complexes exhibit νRu-P stretching in the range 521–511 cm^{-1}. Also, the νRu-S, νRu-N and νRu-O stretching vibrations occur as weak bands in a region of low intensity at about 500–350 cm^{-1} [55].

3.4 Multinuclear $^{31}P\{^{1}H\}$, ^{1}H and ^{13}C NMR experiments

In the ^{1}H NMR spectra of the free ligands, a shoulder band corresponding to a singlet of the N–H group proton is observed in the region of 8.10–8.70 ppm [28, 29, 50]. This kind of signal is absent in the spectra of the complexes, indicating the deprotonation of the acylthioureide group by the coordination of the ligand, which acts as a monoanionic species, to the metal. Additionally, the ^{1}H NMR spectra of complexes 1–4 showed the characteristic deshielded signal at 9.41 and 8.54 ppm, corresponding to the *ortho* hydrogen atoms of the bipy ligand. Other aromatic hydrogen atoms resonances are in the range 6.28–7.94 ppm, which are attributed to the protons present in the triphenylphosphine and bipy, as well as the aromatic H atoms of the *N*-(acyl)-*N',N'*-(disubstituted)thiourea ligands. Complexes 2 and 4 present two distinct signals in the regions of 6.55–6.39 and 6.45–6.29 ppm, which can be attributed to the hydrogen atoms of the furan group. Additionally, complexes 3 and 4 showed

two shielded signals at 4.95–4.90 and 4.74–4.56 ppm, which are assigned to the methylene protons of the N',N'-dibenzyl groups. The ^{13}C NMR spectra of complexes 1–4 show signals at around 177.4–175.5 and 172.6–164.7 ppm, which are assigned to the C⋯S and C⋯O groups, respectively. For the free ligands, these signals occur at about 183 ppm for C=S, and close to 163 ppm for the C=O group, evidencing the coordination of the metal to the ligands through O,S atoms. In the complexes, the shifts of these two peaks to lower (CS) and higher frequencies (CO), respectively, compared with the free ligands, may be attributed to the delocalization of π electrons of the $^{-}$S⋯Ru⋯O chelate rings, accounting for the opposite displacements with respect to the free ligand. The same effect was previously observed for other transition metal complexes containing *N*-(acyl)-*N',N'*-(disubstituted)thiourea ligands [19, 23, 31].

Aromatic carbon atoms were also identified in the range 159–123 ppm. In the spectra of complexes 2 and 4, the signals in the range 118–111 ppm belong to the carbon atoms of the furan group, while the complexes 3 and 4 present signals at around 53–51 ppm, which are assigned to carbon atoms of the CH_2 groups.

The $^{31}P\{^{1}H\}$ experiments show the presence of only one singlet signal for coordinated phosphorus of each complex around 22–21 ppm (Table 2) due to equivalence of the two phosphorus atoms in *trans* configuration [11, 36, 51]. In the $^{31}P\{^{1}H\}$ spectra of complexes 1–4, heptet signals of the PF_6^- anion around -144 ppm were observed.

INSERT TABLE 2

3.5 Electrochemical studies

The electrochemical behaviour of complexes 1–4 in cyclic voltammetric experiments were similar to those found for other Ru(II) complexes that present monophosphine as ligands

in a *trans* configuration [11]. These experiments were performed in the same conditions and it was observed that complexes 1–4 exhibit a *quasi*-reversible redox process assigned to one-electron Ru(II)/Ru(III), with E*pa* ranging from 920 to 958 mV (Table 2). The similar electrochemical behaviour observed for all complexes may be due to the same stereochemistry found for them. Recently, Barbosa *et al.* [11] reported the electrochemistry of the complex *trans*-$[Ru(PPh_3)_2(Lap)(bipy)]PF_6$ (Lap = lapachol), which presents an oxidation process higher than 1.0 V. In this compound, the O–O-chelated lapachol presents two hard oxygen atoms coordinated to the metal centre, whereas in the complexes with acylthiourea ligands, there is one soft (sulfur) and one hard (oxygen) atom coordinated. The oxidation process occurs at a potential lower than 1.0 V because the sulfur atom is a better electron donor than the oxygen. The E½ values found for complexes 1–4 were considerably more anodic than that observed for the precursor $[RuCl_2(PPh_3)_2(bipy)]$ (Table 2), indicating that the ruthenium centre is more stable in the complexes containing the acylthiourea ligands compared with the precursor. Such metal stabilization is assumed to be due to the replacement of two chlorides by a negatively charged chelating ligand.

3.6. Fluorescence spectra of BSA–Ru(II) complexes

Albumin is the most abundant protein in plasma, thus its interaction with complexes 1-4 was evaluated. Complex binding to this protein may lead to reduction or enhancement of their biological properties because this protein presents the ability to transport drugs and nutrients through the organism [56]. BSA solutions exhibit a strong fluorescence emission with a peak at 340 nm when excited at 280 nm, which is provided mainly by two residues of tryptophan: Trp-134, which is located on the surface of domain I, and Trp-213, which is located within the hydrophobic pocket of domain II [56]. The interaction of ruthenium(II) complexes with BSA was studied by a fluorescence quenching experiment. The experiments

were carried out by adding the ruthenium(II) complexes in increasing concentrations (0–100 μM) to BSA (2.5 μM) at 295 and 310 K, then following the decrease in fluorescence intensity (Table 4; Figure 3A).

INSERT TABLE 4

INSERT FIGURE 3

The fluorescence quenching can be illustrated by the well-known Stern–Volmer equation [57]:

$$F_0/F = 1 + K_{sv}[Q] = 1 + k_q\tau_0[Q]$$

where F_0 and F represent the fluorescence intensities of BSA in the absence and presence of the complexes, respectively, K_{sv} is the Stern–Volmer quenching constant, kq is the bimolecular quenching rate constant (units $M^{-1}S^{-1}$). τ_0 is the emission lifetime of the fluorescent biomolecule in the absence of quencher (τ_0 = 6.2 ns) [58] and [Q] is the concentration of the quencher (the Ru(II) complex). The value of K_{sv} is obtained as the slope of the linear plot of F_0/F *vs*. [Q]. In addition, according to $k_q = K_{SV}/\tau_0$, the quenching rate constant k_q can be calculated. The binding constant (K_b) and the number of binding sites (*n*) can be determined using the following equation:

$$\log\frac{(F_0 - F)}{F} = \log K_b + n\log[Q]$$

where K_b is the equilibrium constant to a site and *n* is the number of binding sites per BSA molecule. K_b and *n* values were obtained from the intercept and slope through the double-logarithm regression curve of $\log[(F_0\text{-}F)/F]$ *vs.* log[Q]. The effect of complex 1 on BSA fluorescence intensity is depicted in Figure 3A. Table 4 shows the constant values for the complexes and the ligands $BzBn_2Th$ and $FuBn_2Th$. The ligands $BzPh_2Th$ and $FuPh_2Th$ do not

interact with BSA, highlighting the importance in BSA binding of the *N',N'*-dibenzyl substituent in the free ligand.

The different mechanisms of quenching are usually classified as dynamic quenching and static quenching, and these can be distinguished by their different dependencies on temperature and viscosity. Static quenching refers to the formation of a complex between quencher and fluorophore in the ground state. When increasing the temperature, the BSA-complex formation decreases leading to a decrease in the fluorescence quenching. Dynamic quenching refers to contact between fluorophores and the quencher during the transient existence of the excited state. In this case, the number of collisions depends upon diffusion, and thus higher temperatures increase the fluorescence quenching, and as a result the quenching constant increases [58]. Accordingly, in this paper, the K_{sv} values are reduced when the temperature is increased. Therefore, the static mechanism is responsible for the interactions between the complexes 1–4 and BSA. Furthermore, the maximum scatter collision-quenching constant values, k_q, occur around at 10^{12} $M^{-1}s^{-1}$ for the complexes 1–4, which is higher than maximum kq value for dynamic quenching [k_q of 2×10^{10} $M^{-1}s^{-1}$], indicating the existence of static quenching mechanism [58]. The values of *n* are close to 1, indicating that there is only one binding site in the BSA for each complex.

The thermodynamic parameters (ΔH°, ΔS° and ΔG°) were analysed to evaluate the intermolecular forces involving the molecules of the complex and BSA. As discussed in the X-ray structure analysis, in the solid state, the complexes can present interactions that include hydrogen bonds, van der Waals forces, electrostatic forces and hydrophobic interaction forces. The types of interactions can occur between the BSA and the complexes, and are indicated by the sign and magnitude of the thermodynamic parameters. The values for $\Delta H° > 0$ and $\Delta S° > 0$ implies the involvement of hydrophobic forces in protein binding, $\Delta H° < 0$ and $\Delta S° < 0$ correspond to van der Waals and hydrogen bonding interactions, and $\Delta H° < 0$ and

$\Delta S° > 0$ suggests an electrostatic force [59]. As observed in Table 4, the positive $\Delta S°$ and negative $\Delta H°$ values indicate that electrostatic forces occur in complexes 1–4, which are allowed by the positive charge of the complexes with negative regions of the protein. Furthermore, the negative value of $\Delta G°$ indicates a spontaneous interaction between them. The magnitude of the BSA-binding constant of the complexes 1–4, compared with other Ru(II) complexes reported recently [60], suggests a moderate interaction with BSA molecule. Thus, the molecules of the complexes 1–4 can be stored in protein and released at desired targets.

3.7 DNA binding: UV-Vis spectrophotometric and viscosity studies

All complexes exhibit the same behaviour when ctDNA is added, in which absorption spectra decrease at the rate of about 1–10%, suggesting a weak interaction between complex and DNA. Binding constants, Kb, were calculated according to the equation [61]:

$$[ctDNA]/(\varepsilon_a-\varepsilon_f) = [ctDNA]/(\varepsilon_b-\varepsilon_f) + 1/Kb(\varepsilon_b-\varepsilon_f)$$

in which [ctDNA] is the concentration of ctDNA in base pairs, ε_a is the ratio of the absorbance/[Ru], ε_f is the extinction coefficient of the free Ru(II) complex, and ε_o is the extinction coefficient of the complex in the fully bound form. The ratio of the slope to the intercept in the plot of [DNA]/(εa-εf) *vs.* [DNA] gives the value of Kb, which was calculated from the metal to ligand charge transfer (MLCT) absorption band (λ_{max}) at around 400 nm (Table 5).

INSERT TABLE 5

Slight changes were observed by the addition of ctDNA in the absorption spectra of complexes 1–4 due to low hypochromism and also by the low Kb values compared with those reported in the literature (Kb ranging from 10^{-3} to 10^{-4} M^{-1}) [62–64]. Figure 3B depicts electronic spectra obtained for complex 1, which is similar to those obtained for complexes 2–4. Considering the molecular structure and positive charge of the complexes, electrostatic interactions with ctDNA are expected, involving the negatively charged phosphate groups of DNA. The Kb values found in this report for complexes 1–4 are comparable with those found for $[Ru(tpy)(PHBI)]^{2+}$ and $[Ru(tpy)(PHNI)]^{2+}$ (PHBI = 2-(2-benzimidazole)-1,10-phenanthroline; PHNI = 2-(2-naphthoimidazole)-1,10-phenanthroline; tpy = 2,2′:6′,2″-terpyridyl [65]) and other cationic Ru(II) complexes that bind to DNA through electrostatic interaction [66]. Electrostatic interactions are weaker than the intercalative interactions observed in complexes containing planar ligands (Kb = 10^{-5}–10^{6} M^{-1}) [62], and those formed by hydrogen bonds between complex and DNA [63]. In addition, Kb values of complexes 1–4 are lower than those observed for the classical intercalator ethidium bromide (Kb ≥ 10^{6} M^{-1}) [64].

Complexes 2 and 4 have a slightly higher affinity to ctDNA than complexes 1 and 3, suggesting that, in solution, the oxygen atom from the furan group of the complexes 2 and 4 could interact weakly with ctDNA by hydrogen bonds, increasing the affinity between them. The interaction between the complexes and ctDNA was also evaluated by viscosity experiments, which can provide a good idea of the mode of interaction between the complex and the ctDNA. It is well known that classical intercalators, such as ethidium bromide, lead to an increase in the viscosity of ctDNA because separation of the base pairs occurs to accommodate the intercalator. A covalent DNA-binding mode may cause its fragmentation, thus decreasing the DNA viscosity [43–46]. The ctDNA viscosity did not increase significantly when the concentration of the complexes was increased (See the plot $(\eta/\eta_o)^{1/3}$ *vs.*

[complex]/[DNA] in supplementary information; Fig. S10). These small changes suggest the existence of only weak interactions between the complexes and ctDNA.

3.8 Biological activity

Complexes 1–4 were evaluated against the DU-145 (human prostate carcinoma), A549 (human lung carcinoma) and L929 (normal) cell lines. The IC_{50} values were calculated from the dose-survival curves obtained after 48 h of metallodrug treatment with an MTT assay (Table 6). The complexes reported here are more cytotoxic than the free ligands, highlighting the importance of the metal to the antitumour biological activity. Complex 3 was the most active against DU-145 cells, while complex 1 was the most potent against A549 cells. For comparison, the cytotoxicity of cisplatin was evaluated under the same experimental conditions. The complexes were more active against human DU-145 and A549 cell lines than cisplatin (Table 6). Interestingly, complex 3 was more selective than cisplatin in the human DU-145 cell line.

INSERT TABLE 6

The $FuPh_2Th$ and $FuBn_2Th$ free ligands present activity against DU-145, while $BzPh_2Th$ and $BzBn_2Th$ are inactive up to 200 µM (Table 6), suggesting that the furan group is important for the activity of the free molecule against this tumour cell line. On the other hand, the $BzPh_2Th$ and $FuBn_2Th$ metal-free ligands were active against the L929 cell line, highlighting that the N,N'-dibenzyl improve the activity of these molecules considering normal cells. Considering the A549 cell line, all free ligands were inactive up to 200 µM.

Recently, our research group reported *bis*-triphenylphosphine/Pd(II) complexes with the ligands studied here [31]. The Pd(II) complexes with $BzPh_2Th$ and $BzBn_2Th$ ligands were

inactive against DU-145, MDA-MB-231 and L-929 cell lines, while the complexes with $FuPh_2Th$ and $FuBn_2Th$ were cytotoxic against MDA-MB-231 and L-929 cell lines only, with IC_{50} values ranging from 35 to 70 μM. In these types of Pd(II) complexes, the activity can be attributed to the steric hindrance of the ligands, as well as the presence of the non-coordinated oxygen from the furan group in the molecule of the ligands [31]. In the present report, complexes of ruthenium(II) were very active in the studied cell lines, presenting very low IC_{50} values. These results show that ruthenium(II) complexes with the same ligands are more active than palladium(II) complexes, highlighting the importance of ruthenium(II) compounds as potential anticancer drugs.

The four Ru(II)-based complexes with *N*-(acyl)-*N',N'*-(disubstituted)thiourea ligands were more cytotoxic against DU-145 and A549 tumour cells than L929 normal cells. It is worth mentioning that to realise a structure-activity relationship by changing ligand substituents is not possible, given that the IC_{50} values obtained are very close and the number of complexes studied is too small for this purpose. The DNA-binding studies suggesting weak interactions with the Ru(II) complexes cannot explain their cytotoxic potency. The mechanism of action of the complexes studied in this work may involve targets other than DNA, such as topoisomerase [67].

4. Conclusions

In summary, in this report four new ruthenium(II) complexes containing *bis*-triphenylphosphines, bipyridine and *N*-(acyl)-*N',N'*-(disubstituted)thiourea derivatives as ligands were synthesized and characterized, and their cytotoxicity against A549 and DU-145 cancer cells was evaluated and compared with normal (L929) cells. The crystal structures of the complexes were determined, and showed that the triphenylphosphine ligands were in the *trans* configuration, as suggested by $^{31}P\{^{1}H\}$ NMR experiments. The studies on

complex/BSA binding show a static fluorescence quenching mechanism. The thermodynamic parameters of the complex/BSA binding indicate a spontaneous interaction between these two species and the presence of electrostatic forces between them. This same kind of weak interactions can be suggested by the spectrophotometric titrations and viscosity studies of complex/DNA binding, with low DNA-binding constants and no significant changes in the DNA viscosity. Furthermore, the IC_{50} values against cancer cells (A549 and DU-145) for the complexes are lower than the IC_{50} values of cisplatin (reference drug) and the free ligands. These results reveal that *N*-(acyl)-*N',N'*-(disubstituted)thiourea derivatives coordinated to ruthenium provide good cytotoxicity against tumour cells. In this series of ruthenium(II) complexes, the complexes 2 and 4 interact more strongly with the DNA molecule than complexes 1 and 3, supporting our previous suggestion that the non-coordinate oxygen atom from the furoyl ring can interact directly with this biomolecule. Thus, the fact that the IC_{50} values for the A549 and DU-145 cancer cells for all four complexes were essentially the same suggests that for this series of complexes the mechanism of action may be not only through the DNA, but also through other biomolecules, such as topoisomerase. This study is ongoing in our laboratory to test this hypothesis.

Acknowledgment

We thank the Brazilian Research Council CNPq and FAPESP. CAPES provide financial support to this research by the project CAPES/MES-CUBA 123/11. R.S. Correa thanks FAPESP (2013/26559-4) and CAPES (14267-13-0) for postdoctoral fellowships. Also, K.M. Oliveira thanks FAPESP (2014/04147-9) for doctoral scholarship and A.Alvarez also thanks Capes/MES-CUBA 022451/2013.

Appendix A. Supplementary data

Coordinates and other crystallographic data have been deposited with the deposition codes CCDC 1043557, CCDC 1043558, CCDC 1043559 and CCDC 1043560, for 1, 2, 3 and 4, respectively. Copies of this information may be obtained from The Director, CCDC, 12 Union Road, Cambridge, CB2 1EZ, UK, Fax: +44 1233 336033, E-mail: deposit@ccdc.cam.ac.uk or www.ccdc.cam.ac.uk.

References

[1] M. Bacac, A.C. G. Hotze, K. V. D. Schilden, J. G. Haasnoot, S. Pacor, E. Alessio, G. Sava, J. Reedijk, J. Inorg. Biochem. 98 (2004) 402-412.

[2] M. Gras, B. Therrien, G. Süss-Fink, P. Stepnicka, A. K. Renfrew, P. J. Dyson, J. Org. Chem. 693 (2008) 3419-3424.

[3] W. Kandioller, E. Balsano, S. M. Meier, U. Jungwirth, S. Göschl, A. Roller, M. A. Jakupec, W. Berger, B. K. Keppler, C. G. Hartinger, Chem. Commun. 49 (2013) 3348-3350.

[4] H. Chen, J. A. Parkinson, R. E. Morris, P. J. Sadler, J. Am. Chem. Soc. 125 (2003) 173–186.

[5] A. Bergamo, A. Masi, P.J. Dyson, G. Sava, Int. J. Oncol. 33 (2008) 1281–1289.

[6] J.E. Debreczeni, A.N. Bullock, G.E. Atilla, D.S. Williams, H. Bregman, S. Knapp, E. Meggers, Angew. Chem. Int. Ed. 45 (2006) 1580–1585.

[7] A. Bergamo, C. Gaiddon, J.H.M. Schellens, J.H. Beijnen, G. Sava. J. Inorg. Biochem. 106 (2012) 90–99.

[8] F.R. Pavan, G. Von Poelhsitz, M.I.F. Barbosa, S.R.A. Leite, A.A. Batista, J. Ellena, L.S. Sato, S.G. Franzblau, V. Moreno, D. Gambino, C.Q.F. Leite, Eur. J. Med. Chem. 46 (2011) 5099-5107.

[9] F.B. Nascimento, G. Von Poelhsitz, F.R. Pavan, D.N. Sato, C.Q.F. Leite, H.S.S. Araujo, J. Ellena, E.E. Castellano, V.M. Deflon, A.A. Batista, J. Inorg. Biochem. 102 (2008) 1783-1789.

[10] E.R. dos Santos, M.A. Mondelli, L.V. Pozzi, R.S. Corrêa, H.S. Salistre-de-Araújo, F.R. Pavan, C.Q.F. Leite, J. Ellena, V.R.S. Malta, S.P. Machado, A.A. Batista, Polyhedron 51 (2013) 292–297

[11] M.I.F. Barbosa, R.S. Correa, K.M. de Oliveira, C. Rodrigues, J. Ellena, O.R. Nascimento, V.P.C. Rocha, F.R. Nonato, T.S. Macedo, J.M. Barbosa-Filho, M.B.P. Soares, A.A. Batista, J. Inorg. Biochem. 136 (2014) 33–39.

[12] O. Estevez-Hernandez, J.L. Hidalgo, E. Reguera, I. Naranjo, Sens. Actuators, B 120 (2007) 766–772.

[13] A. Plutin, H. Márquez, M. Morales, M. Sosa, L. Morán, Y. Rodríguez, M. Suárez, C. Seoane, N. Martín, Tetrahedron 56 (2000) 1533 - 1594.

[14] K.R. Koch. Coord. Chem. Rev. 216–217 (2001) 473–488.

[15] H. Pérez, Y.P. Mascarenhas, A.M. Plutin, R.S. Corrêa, J. Duque. Acta Crystallogr. Sect. E, 64 (2008) m503.

[16] H. Pérez, R.S. Corrêa, A.M. Plutin, B. O'Reilly, J. Duque, Acta Crystallogr. Sect. E, 64 (2008) m733-m734.

[17] H. Pérez, R.S. Corrêa, J. Duque, A.M. Plutin, B. O'Reilly, Acta Crystallogr. Sect. E, 64 (2008) m916.

[18] H. Pérez, R.S. Corrêa, A.M. Plutín, O. Calderon, J. Duque, Acta Crystallogr. Section E, 65 (2009) m242.

[19] H. Pérez, R.S. Corrêa, B. O'Reilly, A.M. Plutín, C.C.P. Silva, Y.P. Mascarenhas. J. Struct. Chem. 53 (2012) 921–926.

[20] B. O'Reilly, A. M. Plutín, H. Pérez, O. Calderón, R. Ramos, R. Martínez, R. A. Toscano, J. Duque, H. Rodríguez-Solla, R. Martínez-Alvarez, M. Suárez, N. Martín, Polyhedron 36 (2012) 133–140.

[21] J. Duque, O. Estévez-Hernández, E. Reguera, J. Ellena, R.S. Correa. J. Coord. Chem. 62 (2009) 2804–2813.

[22] N. Gunasekaran, S.W. Ng, E.R.T. Tiekink, R. Karvembu. Polyhedron 34 (2012) 41–45.

[23] S.S. Tan, A.A. Al-abbasi, M.I.M. Tahir, M.B. Kassim, Polyhedron, 68 (2014) 287–294.

[24] B. Schmitt, T.I.A. Gerber, E. Hosten, R. Betz, Inorg. Chem. Commun. 24 (2012) 136–139.

[25] J.G. Małecki, J. Nycz, Polyhedron, 55 (2013) 49–56.

[26] J. Schroer, U. Abram, Polyhedron 28 (2009) 2277–2283.

[27] N. Selvakumaran, S.W. Ng, E.R.T. Tiekink, R. Karvembu, Inorg. Chim. Acta. 376 (2011) 278–284.

[28] W. Hernández, E. Spodine, J. C. Muñoz, L. Beyer, U. Schroder, J. Ferreira, M. Pavani Bioinorg. Chem. Appl., 1 (2003) 271-284.

[29] W. Hernández, E. Spodine, L. Beyer, U. Schröder, R. Richter, J. Ferreira, M. Pavani, Bioinorg. Chem. Appl., 3 (2005) 299-316.

[30] A. Rodger, K.K. Patel, K.J. Sanders, M. Datt, C. Sacht, M.J. Hannon. J. Chem. Soc., Dalton Trans. (2002) 3656–3663

[31] A.M. Plutin, R. Mocelo, A. Alvarez, R. Ramos, E.E. Castellano, M.R. Cominetti, A.E. Graminha, A.G. Ferreira, A.A. Batista, J. Inorg. Biochem. 134 (2014) 76-82.

[32] S. Mihai, M. Negoiu, Rev. Chim., 7 (2012) 63.

[33] N. Gunasekaran, P. Jerome, S.W. Ng, E.R.T Tiekink, R. Karvembu, J. Mol. Catal. A: Chem. (2012) 353–354.

[34] V. Cîrcu, M. Ilie, F. Dumitrascu, I. Neagoe, S. Pasculescu, Polyhedron, 28 (2009) 3739–3746.

[35] J.Sieler, R.Richter, E.Hoyer, L.Beyer, O.Lindqvist, L. Anderson. Z. Anorg. Allg. Chem. 580 (1990) 167-174.

[36] A.A. Batista, M.O. Santiago, C.L. Donicci, I.S. Moreira, P.C. Healy, S.J. Berners-Price, S.L. Queiroz, Polyhedron 20 (2001) 2123-2128.

[37] COLLECT Data Collection Software; Nonius: Delft, 1998.

[38] Z. Otwinowski, W. Minor, In Methods in Enzymology: Macromolecular Crystallography, Part A; Carter, C. W., Jr., Sweet, R. M., Eds.; Academic Press: New York, 1997; Vol. 276, pp 307−326.

[39] G.M. Sheldrick, Acta Crystallogr. Sect. A. 64 (2008) 112−122.

[40] P. Coppens, L. Leiserowitz, D. Rabinovich. Acta Crystallogr. 18 (1965) 1035-1038.

[41] L. J. Farrugia. J. Appl. Crystallogr. 32 (1999) 837-838.

[42] C.F. Macrae, I.J. Bruno, J.A. Chisholm, P.R. Edgington, P. Mccabe, E. Pidcock, L.R. Monge, R. Taylor, J. van de Streek, P.A. Wood, J. Appl. Crystallogr. 41 (2008) 466-470.

[43] G. Cohen, H. Eisenberg, Biopolymers 8 (1969) 45-55.

[44] A. Sellamuthu, R. Ravishankaran, A. A. Karande, M. Kandaswamy, Dalton Trans. 41 (2012) 12970- 12983.

[45] Z. Petra, P. Franc, T. Iztok, G. Gerald, P. Georges, J. Inorg. Biochem. 117 (2012) 35–47.

[46] N. Maribel, C. William, A. R. H-P., S. Anibal, A. M. Jesús, T. Peter, S-D. R. A., J. Inorg. Biochem. 105 (2011) 1684–1691.

[47] T. Mosmann. J. Immun. Meth., 65 (1983) 55-63.

[48] W. J. Geary. Coord. Chem. Rev. 7 (1971) 81–122.

[49] F. T. Martins, R. S. Corrêa, A. A. Batista, J. Ellena. Cryst. Eng. Comm. 16 (2014) 7013–7022.

[50] H. Pérez, R.S. Correa, A.M. Plutin, B. O'Reilly, M.B. Andrade. Acta Crystallogr C. 68 (2012) o19–o22.

[51] N. Gunasekaran, R. Karvembu, S.W. Ng, E.R.T. Tiekink, Acta. Crystallogr. E. 66 (2010) o2572–o2573.

[52] M.G. Woldu, J. Dillen. Theor. Chem. Acc. 121 (2008) 71–82.

[53] R.S. Corrêa, J.P. Barolli, M.I.F. Barbosa, J. Ellena, A.A. Batista. J. Mol. Struct. 1048 (2013) 11–17.

[54] R.S. Corrêa, A.E. Graminha, J. Ellena, A. A. Batista. Acta. Cryst. C67 (2011) m304–m306.

[55] K. Nakamoto, Infrared and Raman Spectra of Inorganic and Coordination Compounds, fourth ed., Wiley, New York, 1986.

[56] F. Xue, C.-Z. Xie, Y.-W. Zhang, Z. Qiao, X. Qiao, J.-Y. Xu, S.-P. Yan. J. Inorg. Biochem. 115 (2012) 78–86.

[57] J.R. Lakowicz, G. Weber. Biochemistry 12 (1973) 4161–4170.

[58] M. Ganeshpandian, R. Loganathan, E. Suresh, A. Riyasdeen, M.A. Akbarshad, M. Palaniandavar. Dalton Trans. 43 (2014) 1203-1219.

[59] P.D. Ross, S. Subramanian. Biochemistry 20 (1981) 3096-3102.

[60] M. Alagesan, P. Sathyadevi, P. Krishnamoorthy, N. S. P. Bhuvanesh, N. Dharmaraj, DaltonTrans. 43 (2014) 15829–15840.

[61] A. Wolfe, G.H. Shimer, T. Meehan. Biochemistry 26 (1987) 6392.

[62] A. Ambroise, B.G. Maiya, Inorg. Chem. 39 (2000) 4256-4263.

[63] Dik-Lung Ma, C.-M. Che, F.-M. Siu, M. Yang, K.-Y. Wong, Inorg. Chem. 46 (2007) 740-749.

[64] U. Chaveerach, A. Meenongwa, Y. Trongpanich, C. Soikum, P. Chaveerach. Polyhedron 29 (2010) 731–738.

[65] C.-W. Jiang, H. Chao, H. Li, L.-N. Ji, J. Inorg. Biochem. 93(2003) 247–255.

[66] C.V. Kumar, J.K. Barton, N.J. Turro, J. Am. Chem. Soc. 107 (1985) 5518–5523.

[67] K. Du, J. Liang, Y. Wang, J. Kou, C. Qian, L. Ji, H. Chao, Dalton Trans. 43 (2014) 17303-17316.

Table 1. Crystal data and structure refinement parameters obtained for the complexes 1–4.

	1	**2**	**3**	**4**
Empirical formula	$[RuC_{66}H_{53}N_4OP_2S]PF_6$	$[RuC_{64}H_{53}N_4O_2P_2S]PF_6$	$[RuC_{68}H_{57}N_4OP_2S]PF_6$	$[RuC_{66}H_{57}N_4O_2P_2S]PF_6$
Formula weight	1258.16	1248.13	1286.22	1276.18
Crystal system	Monoclinic	Monoclinic	Triclinic	Triclinic
Space group	$P2_1$	$P2_1/c$	P-1	P-1
Unit cell dimensions				
a (Å)	12.9440(5)	17.1920(17)	11.6690(5)	12.0148(10)
b (Å)	19.1800(7)	15.9090(16)	12.8000(6)	12.6966(9)
c (Å)	13.2220(9)	20.718(2)	21.2980(13)	20.7902(12)
α (°)	90	90	89.022(2)	88.478(3)
β (°)	115.510(3)	90.591(8)	84.947(2)	83.689(3)
γ (°)	90	90	69.035(2)	67.217(4)
Volume ($Å^3$)	2962.6(3)	5666.2(10)	2958.6(3)	2905.9(4)
Z	2	4	2	2
Density calculated (Mg/m^3)	1.410	1.463	1.444	1.459
μ (mm^{-1})	0.447	0.467	0.449	0.458
F(000)	1288	2552	1320	1308
Crystal size (mm^3)	0.10 x 0.28 x 0.40	0.04 x 0.13 x 0.40	0.06 x 0.12 x 0.32	0.04 x 0.18 x 0.20
θ range (°)	3.09 to 26.37	2.98 to 26.09	2.95 to 26.40	2.96 to 26.38
Index ranges	$-16\leq h\leq 16$, $-23\leq k\leq 23$, $-16\leq l\leq 16$	$-21\leq h\leq 21$, $-19\leq k\leq 19$, $-24\leq l\leq 25$	$14\leq h\leq 13$, $-16\leq k\leq 16$, $-26\leq l\leq 26$	$15\leq h\leq 15$, $-14\leq k\leq 15$, $-25\leq l\leq 25$
Reflections collected	18413	39747	22404	20850
Independent reflections	11477 [R(int) = 0.0478]	11143 [R(int) = 0.0697]	12048 [R(int) = 0.0286]	11790 [R(int) = 0.0389]
Completeness to θ (%)	99.0	99.2	99.4	99.4
Max. and min. transmission	0.95403 and 0.83425	0.98206 and 0.86997	0.98056 and 0.86057	0.98118 and 0.91907
Data / restraints / parameters	11477 / 1 / 739	11143 / 0 / 730	12048 / 0 / 811	11790 / 0 / 802
Goodness-of-fit on F^2	1.016	1.003	1.015	1.138
Final R indices [I>2sigma(I)]	R1 = 0.0485, wR2 = 0.1074	R1 = 0.0556, wR2 = 0.1448	R1 = 0.0404, wR2 = 0.1030	R1 = 0.0617, wR2 = 0.1376
R indices (all data)	R1 = 0.0759, wR2 = 0.1197	R1 = 0.0817, wR2 = 0.1597	R1 = 0.0565, wR2 = 0.1104	R1 = 0.1016, wR2 = 0.1723
$\Delta\rho_{max.}$ and $\Delta\rho_{min.}$ ($e.Å^{-3}$)	0.630 and -0.670	1.056 and -0.696	0.674 and -0.587	0.595 and -0.758

Table 2. $^{31}P\{^{1}H\}$ NMR and cyclic voltammetry data for complexes 1-4 and the precursor $[RuCl_2(PPh_3)_2(bipy)]$.

Complex	**δ (ppm)**	**E*pa* (mV)**	**$E_{1/2}$ (mV)**
1	21.12	920	790
2	21.95	950	901
3	22.07	958	851
4	22.49	924	847
$[RuCl_2(PPh_3)_2(bipy)]$[36]	21.53	420	380

Table 3. Selected bond and angle lengths (Å,°) for 1–4 around the acylthiourea moiety compared with Mogul survey and around the metal center.

Fragment	**1**	**2**	**3**	**4**	**Mogul analysis**
Acylthiourea moiety					*Mean values*
d C1—O1	1.265(6)	1.269(4)	1.268(3)	1.262(5)	1.22(2)
d C2—S1	1.704(5)	1.711(3)	1.716(2)	1.714(4)	1.68(1)
d C1—N1	1.324(6)	1.333(5)	1.331(3)	1.324(6)	1.37(2)
d C2—N1	1.346(6)	1.336(4)	1.332(3)	1.338(5)	1.35(2)
d C2 —N2	1.378(6)	1.362(5)	1.353(3)	1.370(5)	1.32(2)
Metal center					
d Ru1—O1	2.083(4)	2.058(2)	2.078(2)	2.063(3)	
d Ru1—S1	2.322(1)	2.354(1)	2.355(1)	2.368(1)	
d Ru1—N3	2.064(5)	2.054(3)	2.058(2)	2.069(3)	
d Ru1—N4	2.115(3)	2.076(3)	2.075(2)	2.071(3)	
d Ru1—P1	2.431(1)	2.432(1)	2.416(1)	2.432(1)	
d Ru1—P2	2.418(1)	2.417(1)	2.420(1)	2.390(1)	
< O1—Ru1—S1	90.48(9)	90.48(7)	88.73(5)	89.61(8)	
<N3—Ru1—N4	77.91(14)	77.92(12)	78.06(8)	78.14(13)	
< P1—Ru1—P2	176.34(4)	172.16(3)	177.64(2)	178.71(4)	
<O1—Ru1—N3	174.68(14)	171.95(11)	169.69(7)	168.33(12)	
<S1—Ru1—N4	171.90(10)	173.14(8)	179.18(5)	174.77(10)	
<N3—Ru1—P1	89.57(12)	94.05(9)	87.04(5)	89.44(9)	
<P2—Ru1—N4	90.30(10)	89.51(8)	90.54(5)	89.50(10)	
Torsion angle					
O1—C1—N1—C2	2.8(8)	1.8(6)	-1.5(4)	0.8(8)	
C1—N1—C2—S1	-1.0(8)	8.6(6)	-6.7(4)	-11.8(7)	

Table 4. The quenching constants (K_{sv}), (k_q), binding constants (K_b), number of binding sites (n) and the thermodynamic parameters relative of Ru(II) complexes with BSA at different temperatures (295 and 310 K).

Compounds	T (K)	Ksv × 10^4 (M^{-1})	k_q × 10^{12} (M^{-1} s^{-1})	K_b × 10^4 (M^{-1})	n	ΔH° (kJ mol^{-1})	ΔS° (J mol^{-1} K^{-1})	ΔG° (kJ mol^{-1})
1	295	(5.95 ± 0.29)	9.60	(2.64 ± 0.28)	0.94	-1.82	85.23	-26.96
	310	(5.74 ± 0.31)	9.26	(2.62 ± 0.11)	0.94			-28.24
2	295	(6.48 ± 0.16)	10.45	(3.16 ± 0.15)	0.91	-1.99	85.35	-27.17
	310	(6.23 ± 0.01)	10.05	(2.13 ± 0.44)	0.90			-28.45
3	295	(4.03 ± 0.36)	6.50	(0.97 ± 0.07)	0.85	-1.25	87.73	-27.13
	310	(4.02 ± 0.31)	6.48	(0.81 ± 0.01)	0.83			-28.45
4	295	(5.33 ± 0.20)	8.60	(2.10 ± 0.89)	0.88	-1.35	85.91	-26.69
	310	(5.19 ± 0.21)	8.37	(1.85 ± 0.15)	0.82			-27.98
$BzBn_2Th$	295	(3.48 ± 0.04)	5.61	(0.16 ± 0.08)	0.86	-2.38	78.85	-25.65
	310	(3.32 ± 0.03)	5.35	(0.14 ± 0.21)	0.89			-26.83
$FuBn_2Th$	295	(5.62 ± 0.13)	9.06	(1.57 ± 0.20)	0.87	-7.89	64.19	-26.82
	310	(4.81 ± 0.17)	7.76	(1.11 ± 0.17)	0.85			-27.79

*Constants were obtained in order of increasing temperature: 295 and 310 K. The ligands $BzPh_2Th$ and $FuPh_2Th$ do not interact with BSA.

Table 5. DNA binding constant (*K*b), λ_{max} used for the analysis and hypochromicity found the complexes 1–4.

Complex	Kb x 10^4 (M^{-1})	λ_{max}(nm)	Hypochromicity (%)
1	0.52 ± 0.02	406	12
2	1.81 ± 0.30	412	11
3	0.95 ± 0.06	400	1
4	1.82 ± 0.06	398	7

Table 6. IC_{50} values (μM) obtained from cytotoxic assays against DU-145 (human prostate cancer), A549 (human lung cancer) and L929 (normal) cell lines for the complexes 1–4, compared with reference drug, cisplatin.

Compounds	**DU-145**	**A549**	**L929**	**IS[1]**	**IS[2]**
1	0.38 ± 0.16	0.28 ± 0.15	1.55 ± 0.42	4.08	5.54
2	0.46 ± 0.17	0.93 ± 0.42	2.01 ± 0.18	4.37	2.16
3	0.22 ± 0.15	0.68 ± 0.47	2.54 ± 0.41	11.55	3.74
4	0.44 ± 0.17	0.57 ± 0.25	1.07 ± 0.38	2.43	1.88
$BzPh_2Th$	> 200	> 200	> 200	-	-
$FuPh_2Th$	71.36 ± 1.50	> 200	> 200	-	-
$BzBn_2Th$	> 200	> 200	68.02 ± 1.95	-	-
$FuBn_2Th$	45.57 ± 1.51	> 200	82.85 ± 25.88	1.82	-
Cisplatin*	2.00 ± 0.47	11.84 ± 8.68	16.53 ± 2.38	5.92	8.27

* Reference drug. **IS[1]**=IC_{50}L-929/IC_{50}DU-145; **IS[2]**=IC_{50}L929/IC_{50}A549.

Figure Captions

Figure 1. *N*-(acyl)-*N',N'*-(di-substituted)thioureas used as ligands: *N*-benzoyl-*N',N'*-diphenylthiourea ($BzPh_2Th$), *N*-(2-furoyl)-*N',N'*-diphenylthiourea ($FuPh_2Th$), *N*-benzoyl-*N',N'*-dibenzylthiourea ($BzBn_2Th$) and *N*-(2-furoyl)-*N',N'*-dibenzylthiourea ($FuBn_2Th$).

Figure 2. Crystal structure of the complex 4 with selected atoms labeled. For the sake of clarity the counter-ion PF_6^- was omitted and the ellipsoids are represented at 30% of probability.

Figure 3. (A) Emission spectra of BSA (2.5 μM; λ_{ex} = 280 nm) at different concentrations of complex 1 (a= 0; b= 0.78; c= 3.12; d= 12.5; e= 25.0; f= 50.0 and g= 100.0 μM^{-1}) at 310 K. Insert: Plots of F_0/F versus [complex 1]. (B) Changes in the electronic absorption spectra of 1 with increasing concentration of ctDNA. Insert: Plots of $[DNA]/\varepsilon_a-\varepsilon_f$ versus [DNA].

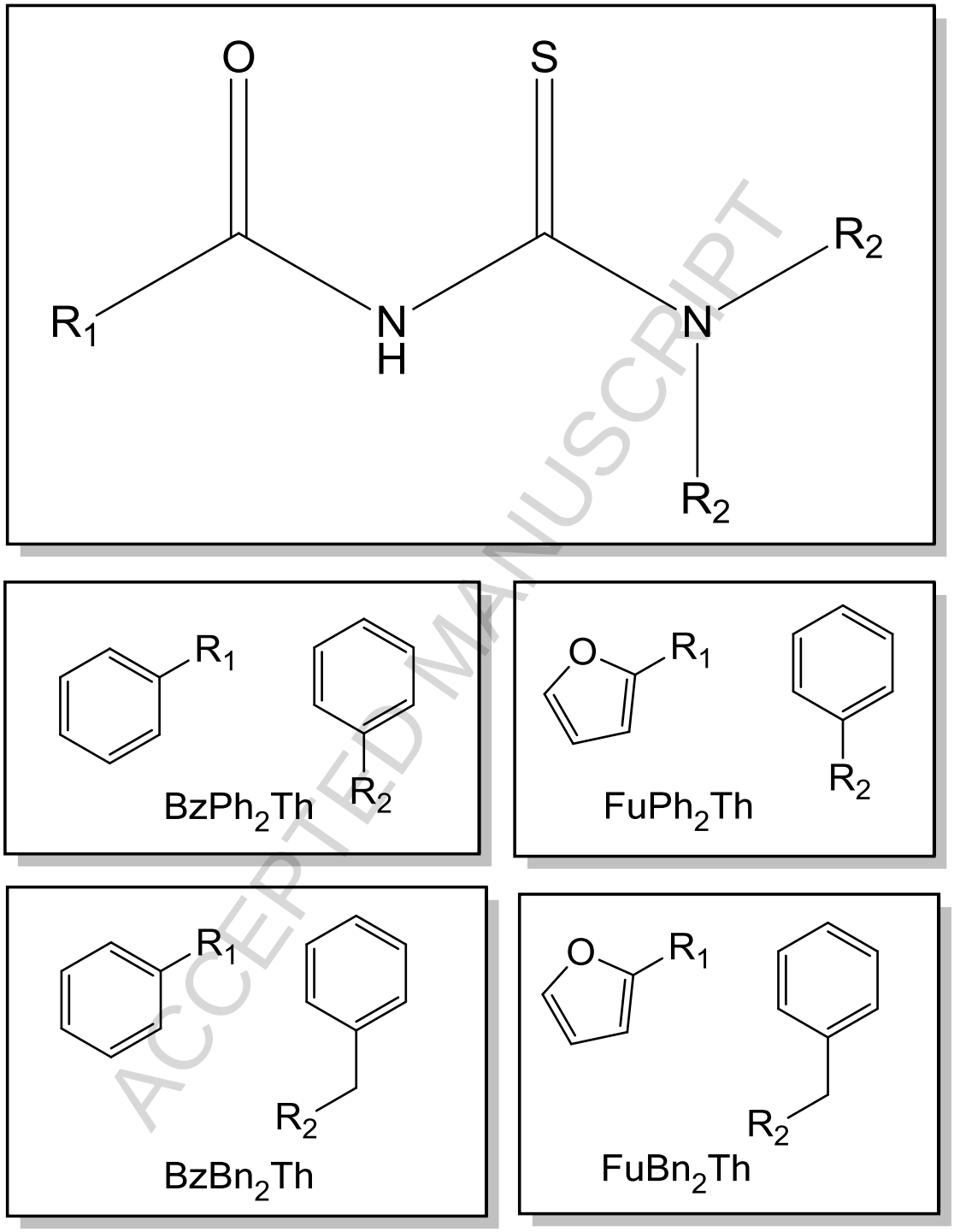

Figure 1

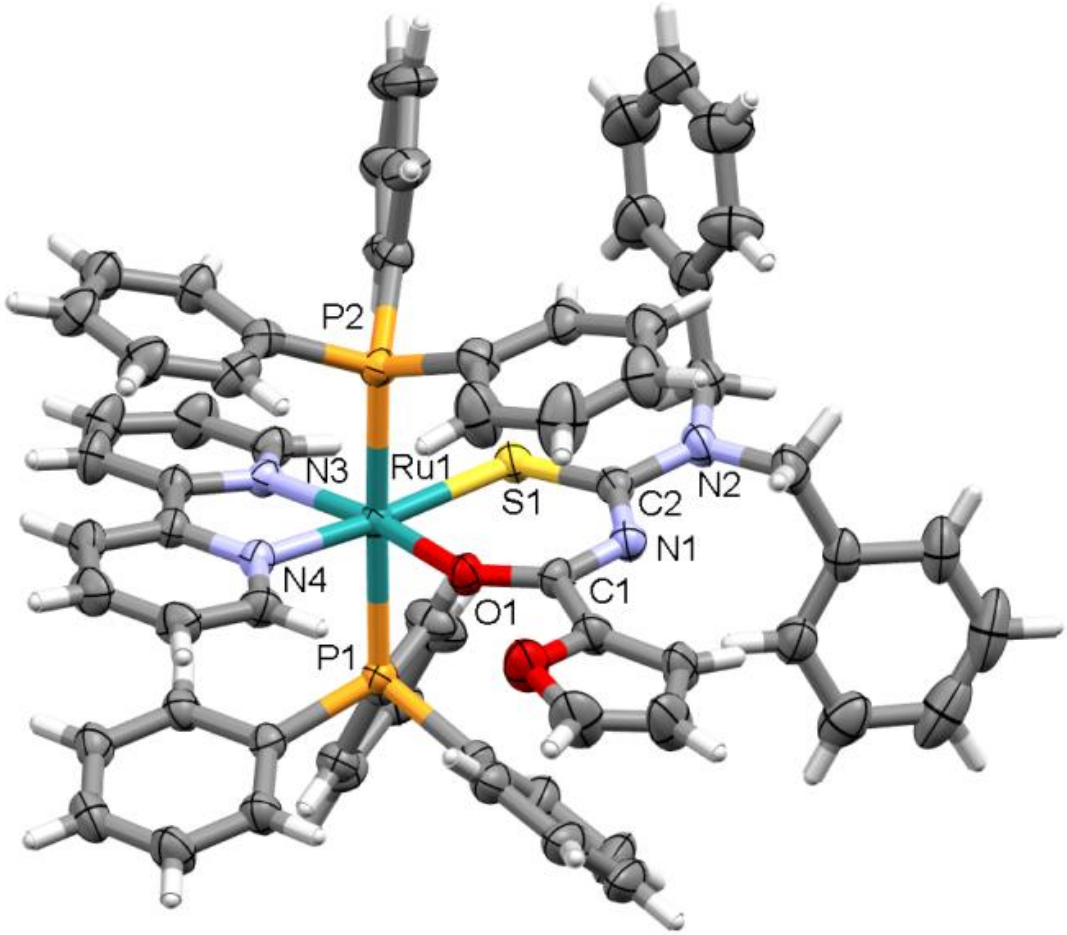

Figure 2

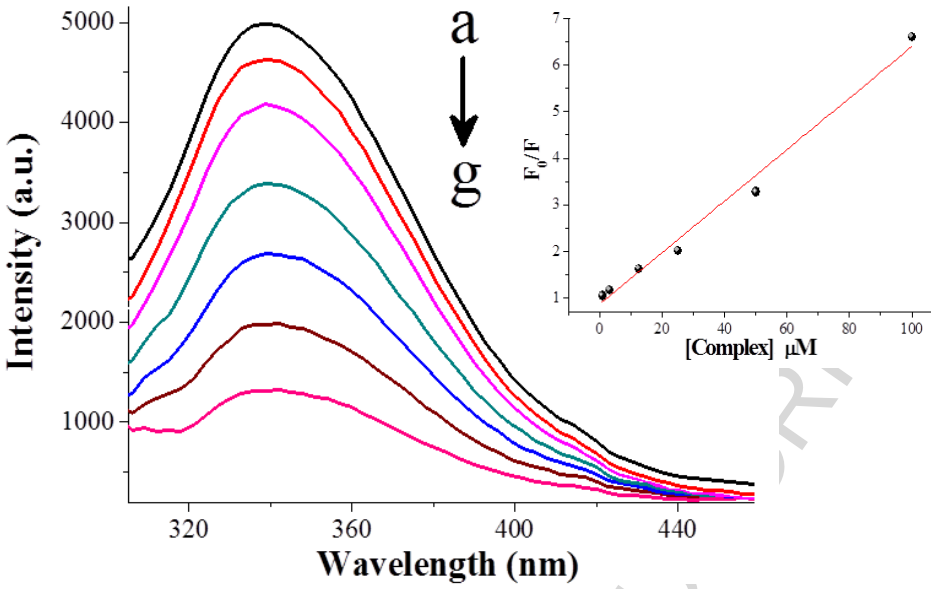

(A)

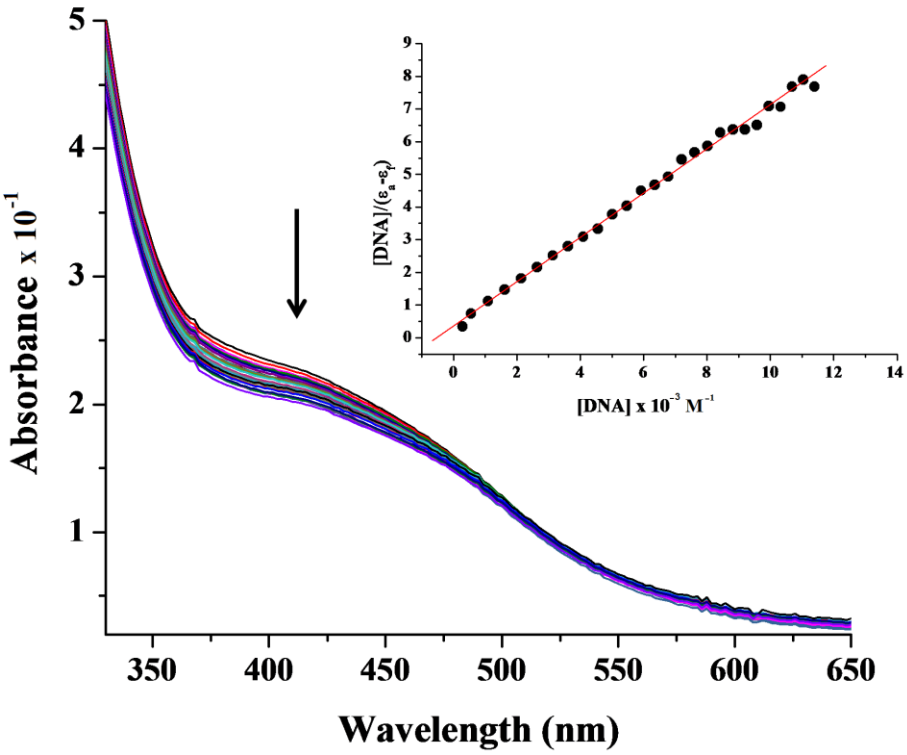

(B)

Figure 3

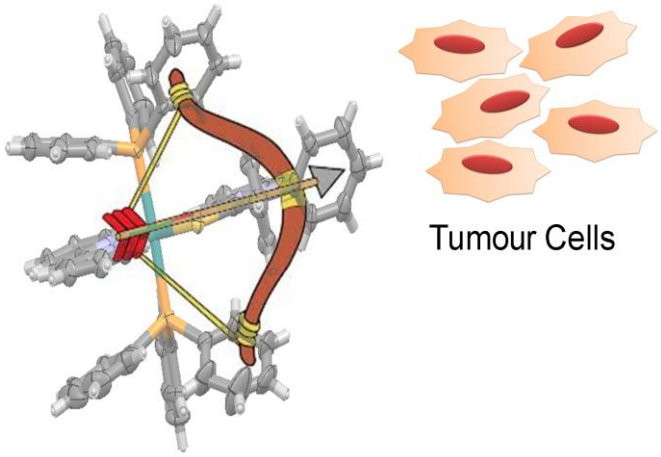

Synopsis: The first examples of complexes of Ru(II) containing *N*-(acyl)-*N*',*N'*-(disubstituted)thioureas were synthesized and characterized. The complexes interact with DNA and BSA mainly by weak electrostatic interactions and they are very active against prostate (DU-145) and lung (A549) tumour cells, and thus are promising anticancer candidates.

Graphical abstract

Highlights:

- Ru(II) complexes with *N*-(acyl)-*N*',*N'*-(disubstituted)thioureas.

- The compounds interact with DNA and BSA by electrostatic interactions.

- Promising agents against prostate (DU-145) and lung (A549) tumour cells.

- High cytotoxic activity against tumour cells than cisplatin.